

# Thermoelectric Property Difference Between Single Crystal and Polycrystalline SnSe

Mi Hongxing<sup>1,2</sup>, Li Huanyong<sup>3</sup>, Qiao Cunyun<sup>4</sup>, Zhang Ting<sup>2</sup>, Han Li<sup>2</sup>, Xu Ju<sup>1,2</sup>

<sup>1</sup> University of Chinese Academy of Sciences, Beijing 100037, China; <sup>2</sup> Micro-nano Fabrication Technology Department, Institute of Electrical Engineering, Chinese Academy of Sciences, Beijing 100190, China; <sup>3</sup> Northwestern Polytechnical University, Xi'an 710072, China; <sup>4</sup> Center for Crystal Research and Development, Technical Institute of Physics and Chemistry, Chinese Academy of Sciences, Beijing 100190, China

**Abstract:** SnSe is a robust candidate for thermoelectric applications due to its excellent  $ZT$  performance. Thermal and electrical properties of single crystal and polycrystalline SnSe were compared. The single crystal sample was synthesized with Bridgeman method, while the polycrystalline sample was synthesized by melting and spark plasma sintering (SPS). The thermoelectric properties of both materials were measured with four-probe method and laser flash method. The results show that power factor of single crystal is twice higher than that of polycrystalline, and thermal conductivity of single crystal is also thrice higher than that of polycrystalline at all temperatures, leading to the highest  $ZT$  value of these two materials. The highest  $ZT$  of single crystal is 0.65 at 823 K, and that is 0.5 at 923 K for polycrystalline.

**Key words:** SnSe; thermoelectric property; single crystal; polycrystalline; thermal conductivity

Thermoelectric (TE) generators can directly convert heat into electricity, with potential applications in waste heat harvesting and TE cooling<sup>[1]</sup>. The conversion efficiency is determined by dimensionless figure of merit,  $ZT=S^2\sigma T/\kappa$ , where  $S$ ,  $\sigma$ ,  $\kappa$  and  $T$  represent Seebeck coefficient, electrical conductivity, thermal conductivity and absolute temperature, respectively<sup>[2]</sup>. According to the Wiedemann-Franz law,  $\kappa\propto\sigma T$ , these parameters are inherently connected, and it is difficult to adjust electrical properties or thermal characteristics independently<sup>[3,4]</sup>. Therefore, semiconductors with intrinsically low thermal conductivity, high electrical conductivity and high Seebeck coefficient are selected for thermoelectric applications<sup>[5]</sup>, such as single crystal  $\text{Bi}_2\text{Te}_3$  and  $\text{PbTe}$ <sup>[6,7]</sup>, alloyed structure LAST<sup>[8]</sup>, nanostructure SiGe compound<sup>[9]</sup> and single crystal tin selenide ( $\text{SnSe}$ )<sup>[10]</sup>. SnSe, with band-gap about 1.0 eV at room temperature,<sup>[11]</sup> has been used for low cost photovoltaics,<sup>[12]</sup> lithium-ion battery anodes<sup>[13]</sup> and memory-switching devices, etc<sup>[14]</sup>.

SnSe is a layered structure distorted like NaCl with Pnma

symmetry at room temperature. A displacive phase transition of Pnma to Cmcm normally occurs at 800 K. In crystal lattice, the strong covalent bond of Sn-Se is aligned along  $b$ - $c$  plane, but the bond formed by the van der Waals forces along (100) plane is weaker, which results in cleavage along this plane. SnSe gets great attraction because of high  $ZT$  value, 2.6 and 2.8 for p- and n-type single crystal along  $b$ -axis, respectively, mainly due to its extremely low thermal conductivity<sup>[10,15]</sup>. However, Ibrahim<sup>[16]</sup> and Pei<sup>[17]</sup> et al mentioned that the thermal transport and density in single crystal are lower than those in polycrystalline crystal, which is against common sense. In order to understand the origin, there is a need to find the discrepancies between single crystalline and polycrystalline SnSe, including synthesis methods, electrical and thermal properties. These researches are very essential for the SnSe thermoelectric applications, but seldom reported in previous studies. In this study, high quality single crystals were grown by vertical Bridgeman method, and the polycrystalline samples were

Received date: July 25, 2019

Foundation item: National Natural Science Foundation of China (51572220); Chinese Academy of Sciences "Hundred Talents" Project

Corresponding author: Xu Ju, Ph. D., Professor, Micro-nano Fabrication Technology Department, Institute of Electrical Engineering, Chinese Academy of Sciences, Beijing 100190, P. R. China, Tel: 0086-10-82547179, E-mail: xuju@mail.iee.ac.cn

Copyright © 2020, Northwest Institute for Nonferrous Metal Research. Published by Science Press. All rights reserved.

synthesized by melting and spark plasma sintering (SPS) method. The highest  $ZT$  value obtained for single crystal and polycrystalline SnSe is 0.65 (823 K) and 0.5 (923 K), respectively.

## 1 Experiment

The melting point of SnSe is 1155.07 K, which is obtained from phase diagram, and verified by thermal gravity analysis (TGA) and differential scanning calorimetry (DSC), as shown in Fig.1<sup>[18,19]</sup>. Sn chunk (9.999%, 24.02 g) and Se shot (99.999%, 16.38 g) were weighed stoichiometrically, then transferred into quartz tube, sealed with flame under high vacuum ( $\sim 10^{-5}$  Pa), placed in a muffle furnace at 1248 K for 24 h, and then cooled down to room temperature. All the operations were carried out in glove box to prevent materials from oxidation.

### 1.1 Single crystal (SC) synthesis

Single crystal growth method has been reported<sup>[10,20-23]</sup>. The sintered SnSe ingot was crushed and sealed in a high-purified double-layered quartz tube. The tube was specially designed with a sharp tip end, then put into a homemade four-section temperature gradient furnace, where the temperature was controlled independently in every section. The charge end was maintained at 1273 K, and the tapered growth end was maintained at 950 K. The temperature gradient for crystal growing region was set to be 2.8 K/cm. The main parameters for growing the single crystal are listed in Table 1. At the beginning, the tube was put into the charge end and kept for 24 h, then moved slowly down through the crystal growing region (1145~1165 K) at a speed of 0.4~0.8 mm/h with zero rotation, and cooled down to room temperature. A high quality single crystal with dimension of  $\Phi 15$  mm $\times$ 45 mm was obtained and cut into cubic trunks along  $a$ -,  $b$ - and  $c$ -axis with diamond wire after orientation. Samples with sizes of 3 mm $\times$ 3 mm $\times$ 10 mm were used for electrical conductivity and Seebeck coefficient test, while samples with sizes 10 mm $\times$ 10 mm $\times$ 2 mm were used for thermal conductivity measurement.

### 1.2 Polycrystal (PC) synthesis

The molten SnSe ingots were crushed and milled on a planetary ball mill at 250 r/min for 3 h using stainless steel vessels filled with  $N_2$ , and the powder was sieved and put in a graphite mold with an inner diameter of 13 mm, sintered by spark plasma sintering (SPS) under pressure of 50 MPa for 5 min, and then a cylinder-shaped sample with 20 mm in height and 13 mm in diameter was obtained. The cylinder was cut into cubic trunks with the same size and the same method as mentioned above parallel to the pressure direction, because  $ZT$  value parallel to pressure direction is higher than that in perpendicular direction<sup>[24]</sup>. Some cut samples are shown in Fig.2.

Phase structure of synthesized crystals and polycrystal was examined by X-ray diffractometer (XRD, Bruker D8 ADVANCE) using Cu K $\alpha$  radiation with  $2\theta$  from 5° to 80°.

Thermal analysis was carried out on Mettler Toledo analytical TGA/DCS analysis. Crystal orientation was measured using the YX-200 model X-ray crystal orientation instrument. Density test was conducted by Archimedes method. The electrical properties were characterized by LSR-3 Linseis four-probe method. Thermal diffusivity  $D_T$  was analyzed by adiabatic model using Netzsch LFA-427; the sample was coated with graphite layer to reduce reflection of laser light and the furnace was filled with argon at a flow rate of 150 mL/min. The specific heat capacity  $C_p$  was measured by DSC data under  $N_2$  atmosphere. The mass density  $\rho$  was obtained by Archimedes method, and the thermal conductivity  $\kappa$  was calculated by  $\kappa = D_T C_p \rho$ .

## 2 Results and Discussion

### 2.1 XRD analysis

Fig.3 shows XRD and corresponding reference diffraction patterns of PC powder and SC orientated samples. The results match the standard Pnma pattern (JCPDS-PDF file NO. 48-1224) and no other phases are found, indicating synthesized sample with pure phase.<sup>[25]</sup> The XRD pattern of the oriented crystal planes matches with standard pattern (200/020) precisely, showing the accurate orientation.

### 2.2 Thermoelectric properties characterization

Fig.4 shows the transport properties of SC and PC samples. The SC samples were tested along  $b$ -axis, and PC samples were measured parallel to the SPS pressure direction.

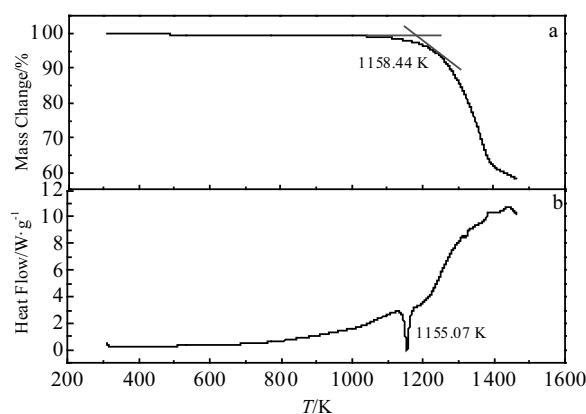


Fig.1 TGA (a) and DSC (b) curves of SnSe under Ar atmosphere<sup>[18,19]</sup>

Table 1 Parameters of SnSe crystal growth

Parameter	Value
Mass of raw material/g	Sn 24.02 Se 16.38
Quartz ampoule size/mm	$\Phi 25$
Vacuum of quartz ampoule/Pa	5~10
Soaking temperature/K	1223
Cooling rate for crystallization/ $K \cdot h^{-1}$	1.2

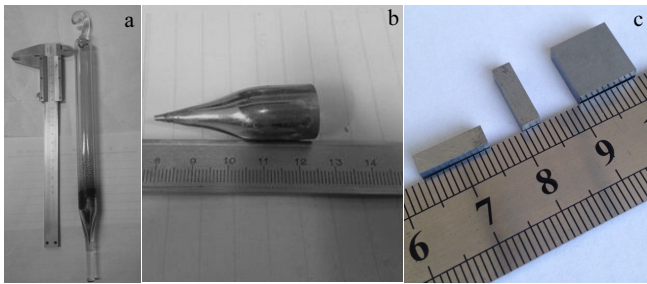


Fig.2 Single crystal SnSe (a, b) and cubic samples (c) cut from crystal for transport properties test (shining face is cleavage planes)

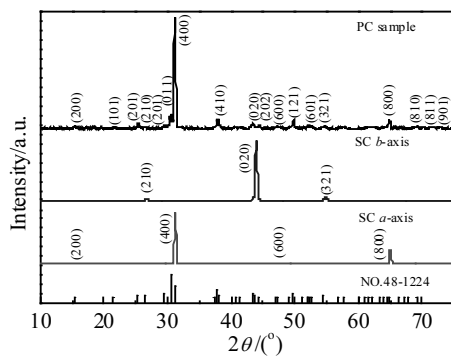


Fig.3 XRD patterns of SnSe powder samples

Electrical conductivity  $\sigma$  is shown in Fig.4a. From room temperature to around 600 K,  $\sigma$  of SC decreases mildly, then increases rapidly to an extremely high point, which is 70.3 S/cm at 823 K for SC. The conversion, from decrease to increase, of  $\sigma$  with temperature represents a transition from metal to semiconductor at about 600 K, which has also been found by Fu et al.<sup>[26]</sup>. For PC sample,  $\sigma$  increases as the temperature rises, reaches the peak of 52 S/cm at 873 K, and there is a platform at about 500 K, showing a similar trend to the SC sample. However, after that, the conductivity of both samples drops sharply, because phase transition from Pnma to Cmcm occurs at around 800 K, leading to decrease of band gap from 0.61 eV to 0.39 eV<sup>[26]</sup>.  $\sigma$  of PC sample is lower than that of SC, mainly because massive dislocations, boundaries and strains restrict the electron mobility and charge concentration.

Seebeck coefficient  $S$  is shown in Fig.4b, and a nearly opposite trend to  $\sigma$  is shown, which can be explained by Eq.(1), and Eq.(2). In the intrinsic excitation region of SnSe, the  $S$  and  $\sigma$  can be expressed as follows:

$$S = k_B(\gamma + C - \ln n) / e \quad (1)$$

$$\sigma = ne\mu \quad (2)$$

where  $n$ ,  $e$ ,  $\mu$ ,  $k_B$ ,  $\gamma$  and  $C$  are the carrier concentration, charge of an electron, electron mobility, Boltzmann

constant, scattering related factor, and a constant number, respectively.  $\sigma$  and  $S$  are oppositely correlated with carrier concentration<sup>[27]</sup>.  $S$  for both sample shows the same trends. The curve goes up slowly to the highest point at about 600 K, and then drops slowly to the valley of 350  $\mu\text{V/K}$  at about 800 K. After that,  $S$  displays a short sharp climbing-up from 800 K to 900 K. The peak and valley value for SC and PC are 583 and 350, 450 and 270  $\mu\text{V/K}$ , respectively. Compared with SC, the  $S$  values for PC are slightly lower, and this difference may be due to variations in the hole concentrations with temperature for PC.<sup>[5]</sup>

The power factor (PF) calculated by the formula  $\text{PF} = S^2\sigma$  is shown in Fig.4c. The trends are similar to  $\sigma$ . With increasing the temperature, PF for SC goes down to the lowest point at 623 K first, and then increases rapidly to the peak of 8.5  $\mu\text{W}\cdot\text{cm}^{-1}\cdot\text{K}^{-2}$  at about 800 K. For PC, there is no concave at 623 K, and the PF curve rises to the peak of 4  $\mu\text{W}\cdot\text{cm}^{-1}\cdot\text{K}^{-2}$  at 873 K, which is only half of that for SC.

Thermal conductivity is calculated from the formula  $\kappa_{\text{total}} = \rho C_D D_T$ ,  $\rho_{\text{SC}} = 6.15 \text{ g}\cdot\text{cm}^{-3}$  and  $\rho_{\text{PC}} = 6.13 \text{ g}\cdot\text{cm}^{-3}$ , both of which are larger than 99% of SnSe theoretical density<sup>[28]</sup>. The total thermal conductivity is calculated by  $\kappa_{\text{total}} = \kappa_l + \kappa_e$ , where  $\kappa_l$  and  $\kappa_e$  are lattice thermal conductivity and electronic thermal conductivity, respectively. The electronic thermal conductivity  $\kappa_e$  can be obtained from Wiedemann-Franz law  $\kappa_e = L\sigma T$  with a Lorenz number  $L$  in the range of  $1 \times 10^{-8} \sim 2.4 \times 10^{-8} \text{ V}^2\cdot\text{K}^{-2}$ . Since  $\sigma$  is less than 100 S/cm, and then  $\kappa_e$  is 4 orders of magnitude smaller than  $\kappa_l$ , so it can be neglected when calculating  $\kappa_{\text{total}}$ . As a result, the measured  $\kappa_{\text{total}}$  can reflect  $\kappa_l$  directly, as shown in Fig.4d~4f<sup>[5, 29]</sup>. The SC thermal conductivity ( $\kappa_{\text{SC}}$ ) first descends slowly as the temperature increases, and then drops from peak value ( $2.5 \text{ W}\cdot\text{m}^{-1}\cdot\text{K}^{-1}$ ) at room temperature to the lowest point ( $1.0 \text{ W}\cdot\text{m}^{-1}\cdot\text{K}^{-1}$ ) at 800 K. Peak and valley value are still larger than those of PC ( $\kappa_{\text{PC}}$ ), and this result is consistent with results from Ibrahim<sup>[16]</sup> and Jin<sup>[30-32]</sup> et al. When the temperature is over 900 K, the value of  $\kappa_{\text{SC}}$  drops sharply, due to the sample expansion. For PC samples,  $\kappa_{\text{PC}}$  decreases as temperature increases, and there is a small hump at phase transition point. All the  $\kappa_{\text{PC}}$  values are below 0.75 since 423 K, and the dropping at about 923 K is the same reason for the deformation (expansion) of the tested sample. Due to the presence of massive defects, boundaries, dislocations for phonon scattering,  $\kappa_{\text{PC}}$  is lower, only half or even one third of  $\kappa_{\text{SC}}$ . Additionally, it is indicated that SnSe is not suitable for application at temperatures over 900 K, because the great deformation happens in both SC and PC.

The dimensionless thermoelectric figures of merit ( $ZT$ ) of all bulk samples are calculated by  $ZT = S^2\sigma T / \kappa_{\text{total}}$  and

the results are shown in Fig.4f. The best  $ZT$  value for SC is 0.65 at 823 K, and PC is 0.5 at 923 K. Because of the volume expansion of the sample, the data is not reliable once the temperature is over 900 K. In the whole temperature range, the SC sample shows larger electrical conductivity, Seebeck coefficient and thermal conductivity than PC, since the single crystals have higher carrier concentration and less crystal defects. However, compared with other single crystal SnSe, we can notice that the reported high  $ZT$  is based on the ultralow thermal conductivity, as listed in Table 2, and many reported  $\kappa$  value of single crystal samples is smaller than that of polycrystalline sample, which needs further study to find

evidence of the lower  $\kappa_{SC}$  compared with  $\kappa_{PC}$ , because massive dislocations, grain boundaries and nanoparticles in polycrystalline sample can act as multi-scale phonon scattering source, leading to thermal conductivity smaller than that of single crystal.<sup>[33]</sup> Our findings in this report are subject to at least three limitations. First, the raw materials used may come from different suppliers; second, single crystal and polycrystal synthesis methods may be different from other reports in detail; and the last, oxidation of the appearance is inevitable during the measurement. More work needs to be done to repeat and to explain transport mechanism and microstructure effect.

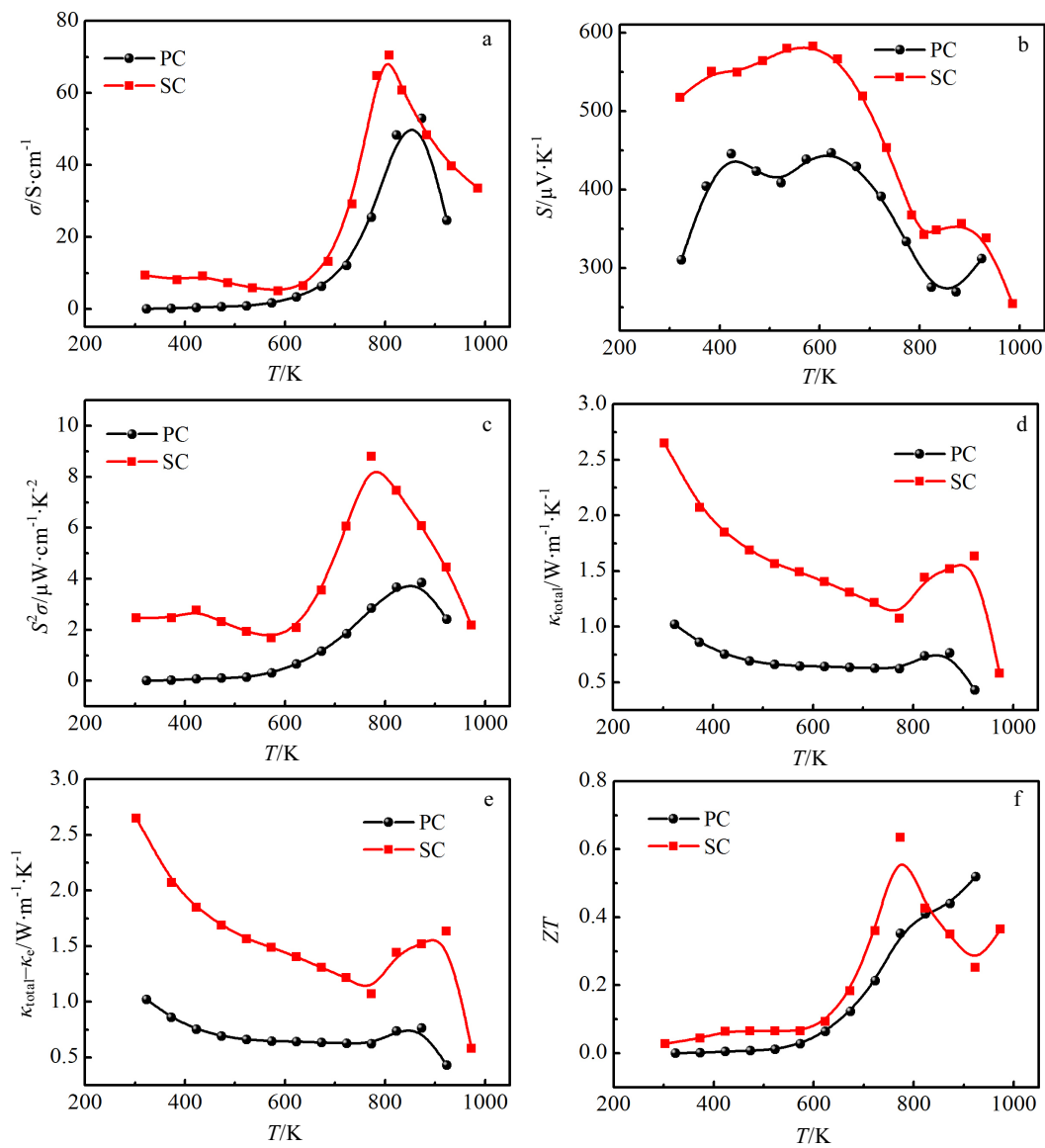


Fig.4 Temperature dependence of the electrical conductivity  $\sigma$  (a), the Seebeck coefficient  $S$  (b), power factor PF (c), total thermal conductivity  $\kappa_{\text{total}}$  (d), lattice thermal conductivity  $\kappa_{\text{total}} - \kappa_e$  (e), and  $ZT$  of SC and PC (f)

**Table 2** *ZT* and  $\kappa$  of single crystal SnSe and non-doped polycrystal SnSe at different temperatures

	<i>ZT</i>	$\kappa/W \cdot m^{-1} \cdot K^{-1}$	<i>T</i> /K	Ref.
Single crystal	2.60	0.35	923	[10]
	2.20	0.20	733	[34]
	2.20	0.60	800	[35]
	1.10	0.25	800	[31]
	0.95	0.50	793	[36]
	0.65	1.10	823	This work
	Polycrystal	1.07	0.75	885
0.50		0.40	773	[38]
0.11		0.80	773	[39]
0.61		0.50	848	[40]
1.10		0.40	873	[41]
0.92		0.50	873	[26]
0.50		0.60	923	This work

### 3 Conclusions

1) Single crystal SnSe has higher electrical conductivity (70.3 S/cm), Seebeck coefficient (583  $\mu$ V/K) and power factor (8.50  $\mu$ W $\cdot$ cm $^{-1}$  $\cdot$ K $^{-2}$ ) than polycrystal SnSe. The calculated power factor of single crystal SnSe is twice higher than that of polycrystal SnSe. Due to the massive defects, boundaries, dislocations in polycrystal, thermal conductivity of single crystal is about thrice higher than that of polycrystal.

2) The highest *ZT* value of 0.65 is obtained at 823 K for single crystal SnSe, and it is 0.5 at 923 K for polycrystal SnSe. Additionally, the density of single crystal and polycrystal samples are both over 99% of theoretical value, and all the samples deform when heated over 900 K.

### References

- Snyder G J, Toberer E S. *Nature Materials*[J], 2008, 7: 105
- Goldsmid H J, Douglas R W. *British Journal of Applied Physics*[J], 1954, 5: 386
- Liu W, Tan X J, Yin K et al. *Physical Review Letters*[J], 2012, 108: 166 601
- Pei Y Z, Shi X Y, LaLonde A et al. *Nature*[J], 2011, 473: 66
- Sassi S, Candolfi C, Vaney J B et al. *Applied Physics Letters*[J], 2014, 104: 212 015
- Kaibe H, Tanaka Y, Sakata M et al. *Journal of Physics and Chemistry of Solids*[J], 1989, 50(9): 945
- Chen Zhigang, Han Guang, Yang Lei et al. *Progress in Natural Science: Materials International*[J], 2012, 22(6): 535
- Hsu K F, Loo S, Guo F et al. *Science*[J], 2004, 303: 818
- Scoville N, Bajgar C, Rolfe J et al. *Nanostructured Materials*[J], 1995, 5(2): 207
- Zhao L D, Lo S H, Zhang Y S et al. *Nature*[J], 2014, 508: 373
- John K J, Pradeep B, Mathai E. *Journal of Materials Science*[J], 1994, 29: 1581
- Zainal Z, Nagalingam S, Kassim A et al. *Solar Energy Materials and Solar Cells*[J], 2004, 81(2): 261
- Jeong J H, Jung D W, Oh E S. *Journal of Alloys and Compounds*[J], 2014, 613: 42
- Agarwal A, Vashi M N, Lakshminarayana D et al. *Journal of Materials Science: Materials in Electronics*[J], 2000, 11: 67
- Chang C, Wu M, He D et al. *Science*[J], 2018, 360: 778
- Ibrahim D, Vaney J B, Sassi S et al. *Applied Physics Letters*[J], 2017, 110: 32 103
- Wei P C, Bhattacharya S, He J et al. *Nature*[J], 2016, 539: 1
- Okamoto H. *Journal of Phase Equilibria*[J], 1998, 19: 293
- Sharma R C, Chang Y A. *Bulletin of Alloy Phase Diagrams*[J], 1986, 7: 68
- Nariya B B, Dasadia A K, Jani A R. *Optoelectronics and Advanced Materials-Rapid Communications*[J], 2013, 7: 53
- Agarwal A, Chaki S H, Lakshminarayana D. *Materials Letters*[J], 2007, 61(30): 5188
- Agarwal A, Vashi M N, Lakshminarayana D et al. *Journal of Materials Science-Materials in Electronics*[J], 2000, 11: 67
- Agarwal A, Patel P D, Lakshminarayana D. *Journal of Crystal Growth*[J], 1994, 142(3-4): 344
- Peng K L, Wu H, Yan Y C et al. *Journal of Materials Chemistry A*[J], 2017, 5: 14 053
- Li Y L, Shi X, Ren D D et al. *Energies*[J], 2015, 8(7): 6275
- Fu Y J, Xu J T, Liu G Q et al. *Journal of Materials Chemistry C*[J], 2016, 4: 1201
- Seo J, Lee D, Lee C et al. *Scripta Materialia*[J], 1998, 38: 477
- Chattopadhyay T, Pannetier J, Vonschnering H G. *Journal of Physics and Chemistry of Solids*[J], 1986, 47: 879
- Chen C L, Wang H, Chen Y Y et al. *Journal of Materials Chemistry A*[J], 2014, 2: 11 171
- Jin M, Shao H Z, Hu H Y et al. *Journal of Crystal Growth*[J], 2017, 460: 112
- Jin M, Shao H Z, Hu H Y et al. *Journal of Alloys and Compounds*[J], 2017, 712: 857
- Wang S, Hui S, Peng K et al. *Applied Physics Letters*[J], 2018, 112: 14
- Dresselhaus M S, Chen G, Tang M Y et al. *Advanced Materials*[J], 2007, 19: 1043
- Duong A T, Nguyen V Q, Duvjir G et al. *Nature Communications*[J], 2016, 7: 13 713

- 35 Peng K L, Lu X, Zhan H et al. *Energy & Environmental Science*[J], 2016, 9: 454
- 36 Jin M, Shao H, Hu H et al. *Journal of Crystal Growth*[J], 2017, 460: 112
- 37 Liu C Y, Miao L, Wang X Y et al. *Chinese Physics B*[J], 2018, 27: 13
- 38 Fu J, Su X, Xie H et al. *Nano Energy*[J], 2018, 44: 53
- 39 Morales Ferreiro J O, Diaz-Droguett D E, Celentano D et al. *Applied Thermal Engineering*[J], 2017, 111: 1426
- 40 Lee S T, Kim M J, Lee G G et al. *Current Applied Physics*[J], 2017, 17: 732
- 41 Popuri S R, Pollet M, Decourt R et al. *Journal of Materials Chemistry C*[J], 2016, 4: 1685

## 单晶和多晶硒化锡的热电性能差异

米红星<sup>1,2</sup>, 李焕勇<sup>3</sup>, 乔存云<sup>4</sup>, 张挺<sup>2</sup>, 韩立<sup>2</sup>, 徐菊<sup>1,2</sup>

(1. 中国科学院大学, 北京 100037)

(2. 中国科学院电工研究所 微纳加工技术与智能电气设备研究部, 北京 100190)

(3. 西北工业大学, 陕西 西安 710072)

(4. 中国科学院理化技术研究所 人工晶体研究发展中心, 北京 100190)

**摘要:** 硒化锡材料因为其优良的热电优值( $ZT$ )性能, 有巨大的热发电应用潜力。对比了单晶和多晶硒化锡在热力学和电输运性能方面的差异。其中, 单晶样品是通过布里奇曼法合成的, 多晶样品则是通过熔融、粉碎和放电等离子烧结 (SPS) 技术合成的。热电性能的测量是通过四探针法和激光闪射法完成的。结果表明: 单晶样品的功率因子是多晶的 2 倍, 而热导率也是多晶样品的 3 倍左右, 这直接导致了单晶和多晶的最高  $ZT$  值差异不大。单晶硒化锡在 823 K 处取得最高热电优值( $ZT$ )为 0.65, 而多晶则是在 923 K 取得最高  $ZT$  为 0.5。

**关键词:** 硒化锡; 热电性能; 单晶; 多晶; 热导率

---

作者简介: 米红星, 男, 1986 年生, 博士生, 中国科学院电工研究所微纳加工技术与智能电气设备研究部, 北京 100190, 电话: 010-82547179, E-mail: mihongxing@mail.iee.ac.cn